Improved performance of railroad ballast using geogrids

Chuhao Liu
Ngoc Trung Ngo
Buddhima Indraratna
Centre for Geomechanics and Railway Engineering, University of Wollongong, Wollongong NSW 2500, Australia
E-mail: cl751@uowmail.edu.au; trung@uow.edu.au; indra@uow.edu.au

ABSTRACT: Geogrids are commonly used to stabilise and reinforce ballast, and over the various laboratory tests have been carried out to determine how geogrids affect the interface between geogrid and ballast aggregates. This paper presents a critical review and interpretation of the results of large-scale direct shear tests and cyclic tests on key parameters such as the interlocking effects of aperture size and the location of geogrids. Field investigations from sites at Bulli and Singleton as well as findings from Discrete Element Modelling, including the influence zone of geogrid and the linear relationship between geometric anisotropy and stress ratio are examined and discussed. It also includes a presentation and discussion of analytical modelling for quantifying the geogrid reinforcing effect (pull-out tests).

Keywords: *Geogrid; Ballast; Rail Transport; Discrete Element Modelling*

1. Introduction

Ballasted rail tracks are the major infrastructure catering for public and freight transport in many countries. Ballast is a free-draining granular medium designed as a load-bearing layer in rail tracks; its main functions are: (i) transmitting induced train loads to the underneath layers at a reduced and acceptable level of stress, (ii) providing lateral resistance, and (iii) facilitating drainage for tracks (Selig and Waters, 1994; Indraratna et al. 2011a). Upon repeated train passage, ballast particles are almost free to move laterally and this leads to the settlement of subgrade soil (foundation). Significant degradation of ballast due to track substructures subjected to large cyclic stresses causes the ballast to become fouled, less angular, and its shear strength decreases (Indraratna et al 2011a). These issues result in excessive track settlement and instability, as well as high maintenance costs.

These problems can be mitigated by utilising planer geosynthetics; three-dimensional cellular reinforcement (geocells) and energy absorbing rubber mats. The ability of geosynthetics to improve track stability has been the subject of numerous experimental and numerical investigations (e.g. Kwon and Penman 2009; Biabani et al2016a; Bathurst and Raymond 1987; Rujikiatkamjorn, et al 2013), among others, all of whom conclude that geosynthetics could stabilise ballast and thus reducing maintenance costs. Fig 1 shows a schematic diagram where geogrid is used in ballasted tracks. Much research has been carried out on geogrid reinforced ballast in order to understand how geogrids interact with particles and how to optimise it as reinforcement. This paper will critically examine how geogrids improve the performance of ballasted tracks. The Authors' assessment is categorised into three main parts: laboratory testing, field investigations, and computational analysis (theoretical aspects and DEM simulations).

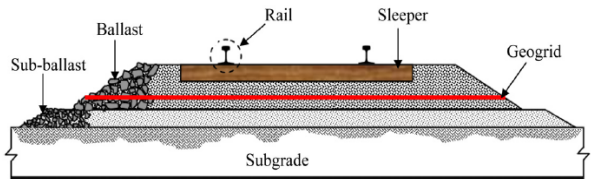

Fig.1 Geogrid reinforced railway (Indraratna et al. 2011)

2. Laboratory Testing

Brown et al. (2007) carried out several full-scale experiments on geogrid reinforced ballast to determine some key factors (aperture size, stiffness, profile of the rib cross section, and location) that influence geosynthetic reinforcement. They find that the aspect ratio (size of aperture to the mean ballast size) helps to quantify the effectiveness of geogrid reinforcement. With 50 mm ballast, 65 mm aperture has the smallest settlement after 3000 cycles loading, which means the optimum aspect ratio is 1.3. Hussaini (2013) also carried out large scale direct shear tests for geogrids with different size apertures; he used the interface efficiency factor (α) previously defined by Koerner (1998) to quantify the degree of reinforcement. This factor is equal to the ratio of the apparent shear strength of the geogrid/ballast interface to the internal shear strength of the ballast, hence:

$$\alpha = \frac{\tan\delta}{\tan\phi} \quad (1)$$

where, δ is the apparent friction angle of the geogrid/ballast interface and ϕ is the internal friction angle of the ballast. Hussaini (2013) reports that with 35 mm ballast the optimum size aperture of geogrid is 42.5 mm, which means the optimum aspect ratio is 1.2 in this case. Although the optimum aspect ratio between these two references is different, they both conclude that the reinforcement became more effective as the aspect ratio increased, but after reaching its optimum point it became less effective as the aspect ratio increased further (Indraratna et al. 2017).

Brown et al. (2007) report that in experiments with a lighter overburden, as the geogrid became stiffer, the extent of reinforcement decreased, but in tests with a higher overburden, stiffer grids showed better reinforcement. They thus concluded that the overburden load needs to be high enough to mobilise the better reinforcement provided by stiffer geogrid because with a lower overburden load, stiffer grids will not deform and will not form good interlocks.

Hussaini et al. (2016) carried out several large-scale cyclic tests that were instrumented by fibre bragg grating

(FBG). They find that the lateral and vertical deformation decreased using geogrids, as was the breakage of ballast. They also report that the optimum location of geogrid for reducing breakage is 130 mm above the subballast. However, Brown et al. (2007) carried out two tests with geogrids at the bottom and mid depth of the ballast layer and one test with two geogrids at the bottom and mid-depth respectively. Their results indicate that the optimum location is at the bottom of the ballast layer, the usual position used in the field, and two geogrid installations did not provide more effective reinforcement. However, Raymond and Ismail (2003) reported that the geogrid should be as close as possible to the bottom of the sleeper and two geogrid layers give better reinforcement than one. Hussaini (2013) reported that the friction angle of the grid/ballast interface decreased with increasing normal stress, as expected.

Indraratna et al. (2011b) carried out several large-scale direct shear tests under different normal stress for ballast and geogrid reinforced ballast. Shear stress-strain results measured in the laboratory are shown in Fig. 2. They report that the peak shear stress of geogrid reinforced ballast is higher than unreinforced ballast for all normal stresses due to the interlocking effect between geogrid and ballast. They also report that while geogrids reduce dilation they have no effect on compression, so they conclude that geogrids restrict the movement of ballast, and reduce dilation (Tutumluer et al 2012; Biabani et al 2016b). As for compression, since the geogrids are thin and flexible, they will not have very much influence on compression. They then carried out tests for ballast with different degrees of fouling and report that the peak shear stress continues to increase as the normal stress increases, but it decreases as the degree of fouling increases. The reason why coal fines reduce the peak stress is because they fill the voids between particles and reduce the particle to particle friction. They said the fines lubricate the ballast and facilitate the particle's rolling and sliding. Therefore, fouling will increase the effect of dilation.

Indraratna et al. (2013) used a novel track process simulation apparatus (TPSA) to investigate the deformation of fouled ballast reinforced with geogrid. The TPSA was modified based on the design of Indraratna and Salim (2003), and the lateral stress ratio used in TPSA was justified by field measurements at the Bulli and Singleton tracks in Australia. As Fig.3 shows, there are three key parts: the horizontal and vertical displacement measure system, the confining stress controlling system, the axial load system, and the prismoidal triaxial chamber. The void contaminant index (VCI) proposed by Indraratna et al (2010a) is used to quantify the degree of fouling, as shown below

$$VCI = \frac{1+e_f}{e_b} \times \frac{G_{sb}}{G_{sf}} \times \frac{M_f}{M_b} \times 100 \quad (2)$$

where, e_f is the void ratio of fouling material, e_b is the void ratio of the fresh material, G_{sb} is the specific gravity of the fresh material, G_{sf} is the specific gravity of the fouling material, M_f is the dry mass of fouling material, and M_b is the dry mass of fresh material.

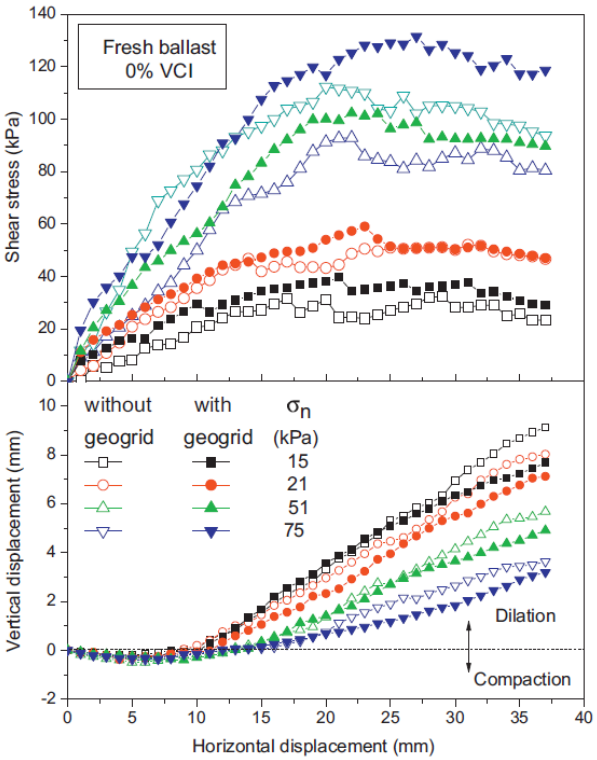

Fig.2 Direct Shear Test Results (Indraratna et al. 2011b)

The lateral and vertical displacement of fresh and fouled ballast with and without geogrid inclusion were measured during the test and revealed that the geogrid reduced the lateral and vertical displacement because the particles over geogrid are compressed and penetrated partially into apertures to create an interlock between ballast and geogrid. This interlock acts as an internal non-horizontal deformed boundary that stops the particles from moving freely (Ngo et al. 2017a, Indraratna et al 2016). This increase in the VCI leads to an increase in lateral displacement as the coal fines coat the particles and inhibit surface contact between them. These fouling materials could provide a lubricating effect that helps the particles roll and slide over each other. They also measured the vertical displacement via the linear variable differential transformer (LVDT) and settlements pegs and found that geogrid reduced the settlement of fresh ballast while all the fouled ballast and fresh ballast reinforced with geogrid had the smallest settlement. They also reported that all the samples settled rapidly during the initial 100,000 cycles, began to gradually deform within 300,000 cycles, and then reached relatively stable settlement towards the end of cyclic loading (500,000 cycles). They believe this phenomenon indicates that in the first range of cyclic loading the ballast is rearranged and becomes denser, but after reaching a certain degree of compression, any further loading cannot cause further settlement, it only promotes dilation. They also report that in terms of the effect of the VCI, the geogrid reduced the settlement of the fresh ballast quite significantly (a 52% and 32% decrease in terms of lateral and vertical deformation). However, an increase in the VCI decreases this reduction because when the VCI equals 40%, the reduction in lateral and vertical displacement decreased by 12% and 5% respectively. Beyond this point of fouling, the effect of geogrid can be omitted so they

concluded that 40% VCI is the threshold value, beyond which geogrid has almost no reinforcing effect on ballast and will cause premature dilation. They therefore recommended this value as a guide for track maintenance. They also carried out a DEM simulation to further understand the deformation of fouled ballast and the compare it with the lab results.

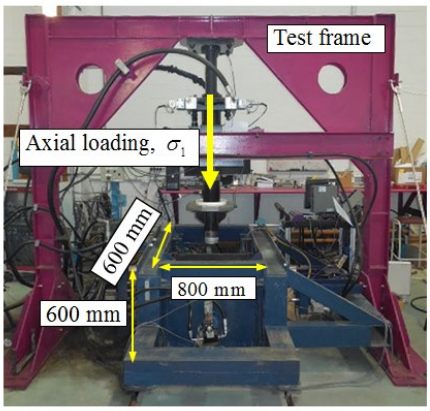

Track Process Simulation Apparatus (TPSA)

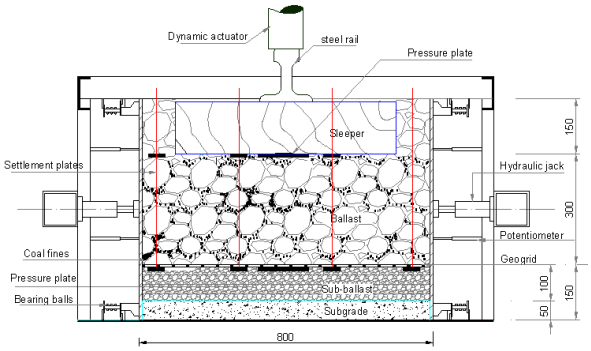

Fig.3 View of TPSA (modified after Indraratna et al. 2013-with permission from ASCE)

3. Field Investigations

Indraratna et al. (2010a) carried out a field investigation at Bulli, New South Wales, Australia to study the benefit of installing a layer of geosynthetics at the interface between ballast and sub ballast and also compare the behaviour of recycled graded ballast and uniform fresh ballast. They installed settlement pegs, displacement transducers, and pressure cells to measure the lateral and vertical displacement, as shown in Fig.4. Since the settlement of graded recycled ballast is less than uniform fresh ballast, their field measurements show that geosynthetics can reduce the lateral displacement of fresh ballast by a large amount and recycled ballast reinforced with geosynthetics performed as well as fresh ballast without geosynthetic reinforcement. They also concluded that installing a geocomposite layer at the interface between ballast and capping can provide internal confinement and thus reduce the maintenance costs.

Indraratna et al. (2014) reported their field investigations at Singleton where they measured the vertical strains of ballast reinforced by three types of geogrids and the long term and transient strain of geogrids against time with strain gauges. Their measurements indicate that the reinforcing effect of geogrids is mainly controlled by their geometric and mechanical properties and the type of subgrade. They also find that geogrids reduced vertical settlement by around 35%, thus indicating the apparent benefits of reducing maintenance costs. They conclude that the optimum size of geogrids with the smallest amount of ballast deformation is 1.1 D_{50}.

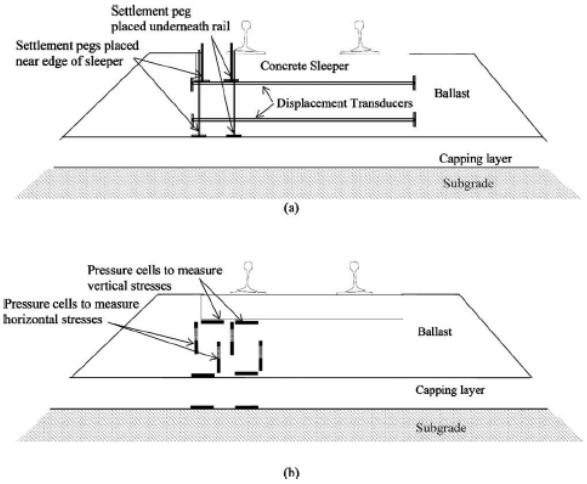

Fig.4 (a) Placement of settlement pegs and displacement transducers; (b) Placement of pressure cells (Indraratna et al. 2010a- with permission from ASCE)

4. Discrete Element Modeling

Cundall and Strack (1979) proposed a distinct element method to model the mechanical behaviour of the particles assemblies. They developed this method by modelling the interaction between particles in contact and the motion of each particle. They then validated this method by comparing the force vector plots from this simulation from a program called BALL with those from a photoelastic analysis, and concluded that this method predicts the behaviour of these assemblies very well. DEM has been used by Lim and McDowell 2005; Ngo et al 2017b; Huang et al. 2009; Indraratna et al. 2014b, among others to model the behaviour of ballast. McDowell et al. (2006) developed a discrete element model to simulate the pull-out test and cyclic triaxial test for ballast reinforced by geogrid. They began by simulating unreinforced ballast in a large-scale triaxial test and then validating the results using reported by Indraratna et al. (1998). They considered angularity by using clumps consisting of several overlapping spheres to model the real shapes of ballast. After comparing the DEM results and the results from the experiments they found that 0.8 was the value of inter-particle friction that matched the real shear strength of ballast in the experiments. However, dilation did occur in some cases, which conflicted with compression in the experiments, but they said this is probably caused by the ballast not breaking in DEM. They carried out several DEM simulations with four aspect ratios (1.6, 1.4, 1.1 and 0.9) in the pull-out tests under the same 0.5 kN surcharge and found the simulation with an aspect ratio of 1.4 had the highest pull-out force at the smallest strain; they concluded that 1.4 is the optimum aspect ratio for this case. They also found that the average shear contact force reached its maximum point at the geogrid and then disappeared 20 cm above and below it, and thus

concluded that the maximum reinforcing effect provided by geogrid is 20 cm above and below it. Finally, they simulated a cyclic triaxial test with three layers of geogrid, and then developed a force ratio β to quantify the effect of reinforcement. It is defined as the ratio of the average contact force in a cuboid 1 cm above and below the four intact apertures in the geogrid to the average contact force in the cuboid 2 cm above and below the entire cross section. Therefore, according to the variation of β, there were strong contacts in the middle of two geogrids during unloading.

Ngo et al (2014) used DEM to simulate large-scale direct shear tests for fresh and foul ballast reinforced with geogrid. They also used the Void Contaminant Index (VCI) defined by Indraratna et al. (2010b) to quantify the degree of fouling and found that fouled ballast will reduce the number of broken bonds, which agrees with the experiment. Ngo et al. (2014) reported that the DEM simulations show that the maximum strain of the geogrid with a 40% VCI of fouled ballast is less than in the fresh ballast because the coal fines increase the amount of contacts between particles and geogrid, thus reducing the interlocking effect between ballast and geogrid.

Chen et al. (2014) used DEM to simulate large box pull out tests, but unlike McDowell et al. (2006) they modelled geogrids by bonding several small balls together with contact and parallel bonds, and also developed a new model to combine two layers of small balls by parallel bonds. They used four types of clumps (2-ball, 4-ball, 8-ball tetrahedral and 8-ball flaky) to simulate the disposal angle. This approached was also used by Ngo et al. 2016, and Hang et al 2010. The critical state angle for the disposal of ballast should be a function of the inter-particle friction angle and angularity. According to Kwan (2006), they chose 0.6 as the particle-particle coefficient of friction and also simulated 20 mm diameter spheres for comparison. The disposal angle in the DEM simulations showed that the disposal angles of the 2-ball and 4-ball clumps are consistent with the real disposal angle of around 40°. The disposal angles of 8-ball tetrahedral and 8-ball flaky are greater than 40° because there are some large voids in the ballast caused by the extra interlock of the complex shape. The simulation results agree with the results of the experiments, especially for the initial 20 mm displacement. They also deduced from the DEM simulations that the shape factor has almost no influence on the initial 20 mm displacement.

Sufian et al. (2017) used DEM to study how the anisotropy of the contact networks influence the internal friction angle. They divided all the contact networks into four sub-networks; strong and non-sliding, strong and sliding, weak and non-sliding, and weak and sliding. The strong and weak contacts are defined by the mean inter-particle contact force (Radjai et al. 1998, Thornton and Antony 1998; Hanatel 2011). If the contact force of this contact is higher than the mean inter-particle contact force it belongs to the strong contact, but according to Alonso-Marroquín et al. (2005), the contact with the friction force that equals the product of the inter-particle coefficient of friction times the normal contact force belongs to the sliding contact. So by calculating the contribution made by four kinds of contact sub-networks they found that the shear resistance comes mainly from the geometric anisotropy of the strong and non-sliding contact sub networks, denoted as $a_c^{s\eta}$. They therefore concluded that the strong and non-sliding sub-networks formed an almost solid structure that forms the main shear resistance, while other three contact networks formed a fluidic structure to form the mean stress. They also found that a unique linear relationship between the geometric anisotropy of the strong and non-sliding sub-networks and the macroscopic stress ratio, as follows:

$$\frac{q}{p} = 0.4 a_c^{s\eta} \tag{3}$$

5. Theoretical Analysis

Teixeira et al. (2007) reported that the pullout resistance has two parts, where one is passive resistance from the transverse ribs and another is the shear resistance between the soil and the surface of the longitudinal and transverse ribs.

Jewell et al. (1984) developed an analytical model to calculate the pull-out force; their theory has two parts, the skin friction between the soil and the reinforcement plan and the other is the bearing force mobilised by the transvers ribs in grids. They assumed that these two parts are independent and additive and the maximum reinforcement is equals to a fully rough sheet where the friction angle is equals to soil's friction angle. Thus, the pull-out force can be calculated as:

$$P = 2LW\sigma_n' f_b \tan\phi \tag{4}$$

where, L the length of the geogrid, W is is the length of the geogrid, σ_n' is the effective normal stress at the geogrids surface, f_b is the bond coefficient which is limited between 0 and 1. When it is equal to 1, the pull-out force will reach its maximum, and the skin friction part of the pull-out force is described as:

$$P_{sf} = 2\alpha_s LW\sigma_n' \tan\xi \tag{5}$$

where, α_s is a fraction of the area of the reinforcement plan, ξ is the friction angle between the surface of the geogrid and the soil. The bearing stress part is determined as:

$$P_{bs} = \left(\frac{L}{S}\right) W \alpha_b B \sigma_b' \tag{6}$$

where, S is the size of the geogrid aperture, so $\frac{L}{S}$ means the number of bearing surfaces in one strip, B is the thickness of the grids, α_b is the fraction of available bearing area in the total area WB, and σ_b' is the effective stress normal to the bearing surface of the ribs. Jewell et al. (1984) developed an equation of a lower estimate of this stress, as given by:

$$\frac{\sigma_b'}{\sigma_n'} = \tan\left(\frac{\pi}{4} + \frac{\phi}{2}\right) exp\left[\left(\frac{\pi}{2} + \phi\right)\tan\phi\right] \tag{7}$$

Equation 7 shows that σ_b' depends solely on the friction angle of soil, which is unreasonable so Jewell (1990) said the particle size is also an important factor that will influence this parameter. He found out that when $B/D_{50} < 10$, D_{50} is the mean particle size of soil and σ_b' will

decrease with increasing B/D_{50}, so when $B/D_{50} > 10$, it will remain constant, as defined by:

if $B/D_{50} < 10$

$$\frac{\sigma_b'}{\sigma_n'} = \left(\frac{\sigma_b'}{\sigma_n'}\right)_\infty \left(\frac{20 - B/D_{50}}{10}\right) \quad (8a)$$

and if $B/D_{50} > 10$

$$\frac{\sigma_b'}{\sigma_n'} = \left(\frac{\sigma_b'}{\sigma_n'}\right)_\infty \quad (8b)$$

Palmeira and Milligan (1989) reported that reducing the space between the bearing ribs decreased the maximum pull-out force due to interference between thee bearing members. They therefore defined a term called the degree of interference which is quantified by comparing the pull-out force of the geogrid and the ideal maximum pull-out force upon which each grid acts as an isolated grid without interacting with each other, hence

$$DI = 1 - \left(P_p / nP_0\right) \quad (9)$$

where, DI is the degree of interference, P_p is the maximum pull-out force for geogrid, n is the number of grids, P_0 is the maximum pull-out force for a single aperture. They then suggested the probable empirical equation to calculate DI should consider the number of bearing members in the geogrid, and the size and thickness of the apertures. Jewell (1990) developed the following equation

$$DI = \left(1 - \frac{1}{n}\right)\left(1 - \frac{(S/\alpha_b B)}{(S/\alpha_b B)_\phi}\right) \quad (10)$$

where, $(S/\alpha_b B)_\phi$ means the ideal condition that makes f_b reach its maximum limit, which is 1. Note that DI increases with an increasing number of ribs, so where there are more ribs, there will be a greater difference between one of apertures in the geogrids and an isolated aperture. According to the second part of Equation 9, DI decreases as the size of the aperture increases, and increases as the geogrid becomes thicker. Because of the degree of interference, Palmeira and Milligan (1989) modified the equation of calculating bond coefficient as below

$$f_b = (\tan \xi_{sr} / \tan \phi)$$

$$f_b = (1 - DI)(B/S)(\sigma_b'/2\sigma_n' \tan \phi) \quad (11)$$

where ξ_{sr} is the equivalent friction angle between soil and geogrid, ϕ is the friction angle of soil.

6. Conclusions

This paper reviewed how geogrids improved the performance of ballast, as carried out in the laboratory, in field investigations, in DEM simulations and by theoretical analysis. The laboratory experiments revealed several results of large-scale direct shear tests and cyclic triaxial tests, where the key parameters that influence the reinforcing effect were discussed from recent literature. In the second part, several studies on using DEM simulate pull-out tests and direct shear tests were reviewed, and the new findings of a correlation between anisotropic geometry and the stress ratio were reviewed and discussed. This approach is a promising way to do research on the interaction between geogrid and particles. In the last part, theoretical analysis of pull out tests were presented and improvements to the original analytical equation were also introduced. This analytical model is very important for understanding and quantifying the mechanism of geogrid/soil interaction.

Acknowledgements

The authors greatly appreciate the financial support from the Rail Manufacturing Cooperative Research Centre (funded jointly by participating rail organisations and the Australian Federal Government's Business Cooperative Research Centres Program) through Project R2.7.1 – The performance of stabilized ballast in rail tracks. The author would also like to thank A/Prof Cholachat Rujikiatkamjorn for his guidance and support at various times. The Authors are also grateful to UOW technical staff, namely, Mr. Alan Grant, and Mr. Cameron Neilson for their assistance during the laboratory study.

References

Alonso-Marroquín, F., Luding, S., Herrmann, H. J. Vardoulakis, I. (2005). Role of anisotropy in the elastoplastic response of a polygonal packing. Phys. Rev. E 71, 5, 1–18.

Bathurst, R.J. and Raymond, G.P. (1987). Geogrid reinforcement of ballasted track. Transportation Research Record, 1153, 8-14.

Biabani, Indraratna, and Ngo, N.T. (2016a). Modelling of geocell-reinforced subballast subjected to cyclic loading. Geotextiles and Geomembranes, 44(4), 489-503.

Biabani, M.M., Ngo, N.T. and Indraratna, B. (2016b). Performance evaluation of railway subballast stabilised with geocell based on pull-out testing. Geotextiles and Geomembranes, 44(4), pp: 579-591.

Brown, S. F., Kwan, J., & Thom, N. H. (2007). Identifying the key parameters that influence geogrid reinforcement of railway ballast. Geotextiles and Geomembranes, 25(6), 326-335.

Chen, C., McDowell, G. R., & Thom, N. H. (2014). Investigating geogrid-reinforced ballast: Experimental pull-out tests and discrete element modelling. Soils and Foundations, 54(1), 1-11.

Cundall, P. Strack, (1979). A discrete numerical model for granular assemblies. geotechnique, 29(1), 47-65.

Huang, H., Tutumluer, E., Hashash, Y.M.A. and Ghaboussi, J. (2009). Discrete element modeling of aggregate behavior in fouled railroad ballast. Geotechnical Special Publication, 192, 33-41.

Hussaini, S. K. K., Indraratna, B., & Vinod, J. S. (2016). A laboratory investigation to assess the functioning of railway ballast with and without geogrids. Transportation Geotechnics, 6, 45-54.

Hussaini, S. K. K. (2013). An Experimental Study on the Deformation Behaviour of Geosynthetically Reinforced Ballast. PhD thesis, University of Wollongong,

Indraratna, Salim, (2003). Deformation and degradation mechanics of recycled ballast stabilised with geosynthetics. Soils and Foundations, 43(4), 35-46.

Indraratna, B., Ionescu, D., & Christie, H. D. (1998). Shear behavior of railway ballast based on large-scale triaxial tests. Journal of geotechnical and geoenvironmental Engineering, 124(5), 439-449.

Indraratna, B., Nimbalkar, S., Christie, D., Rujikiatkamjorn, C., & Vinod, J. (2010a). Field assessment of the performance of a ballasted rail track with and without geosynthetics. Journal of Geotechnical and Geoenvironmental Engineering, 136(7), 907-917.

Indraratna, B., Salim, W. and Rujikiatkamjorn, C. (2011a). Advanced Rail Geotechnology - Ballasted Track, CRC Press, Taylor & Francis Group, London, UK

Indraratna, B., Ngo, N.T. and Rujikiatkamjorn, C. (2011b). Behavior of geogrid-reinforced ballast under various levels of fouling. Geotextiles and Geomembranes, 29(3), 313-322.

Indraratna, Nimbalkar, Tennakoon, (2010b). The behaviour of ballasted track foundations: track drainage and geosynthetic reinforcement. In GeoFlorida 2010: Advances in analysis, modeling & design, 2378-2387).

Indraratna, B, Ngo,N.T and Rujikiatkamjorn, C. (2013). Deformation of coal fouled ballast stabilized with geogrid under cyclic load. Journal of Geotechnical and Geoenvironmental Engineering 139.8, 1275-1289.

Indraratna, B., Nimbalkar, S., & Rujikiatkamjorn, C. (2014). Enhancement of rail track performance through utilisation of geosynthetic inclusions. Geotech. Eng. Jl. of the SEAGS & AGSSEA, 45(1), 17-27.

Indraratna, B., Ngo, N.T., Rujikiatkamjorn, C. and Vinod, J. (2014b). Behaviour of fresh and fouled railway ballast subjected to direct shear testing - a discrete element simulation. International Journal of Geomechanics, ASCE, 14(1), pp: 34-44.

Indraratna, B., Nimbalkar, Ngo, N.T., Neville, (2016). Performance improvement of rail track substructure using artificial inclusions– Experimental and numerical studies. Transportation Geotechnics, 8, 69-85.

Indraratna, B., Sun, Q., Ngo, N.T. and Rujikiatkamjorn, C. (2017). Current research into ballasted rail tracks: model tests and their practical implications. Australian Journal of Structural Engineering, pp: 1-17.

Jewell, R. A. (1990). Reinforcement bond capacity. Geotechnique, 40(3), 513-518.

Jewell, R.A., Milligan, G. W. E., Sarsby, R. W., and DuBois, D. (1984). Interaction between soil and grids. Polymer Grid Reinforcement, 18-30, Thomas Telford.

Han, J., Bhandari, A. and Wang, F. (2011). DEM analysis of stresses and deformations of geogrid-reinforced embankments over piles. International Journal of geomechanics, ASCE, 12(4), pp: 340-350

Huang, H., Tutumluer, E., Hashash, Y.M.A. and Ghaboussi, J. (2010). Discrete element modeling of coal dust fouled railroad ballast behavior. the 89th Annual Meeting DVD of the Transportation Research Board, Washington, DC.

Koerner, R. M. (1998). Designing with geosynthetics, 4th ed., New Jersey: Prentice Hall.

Kwan, C.C., 2006, Geogrid Reinforcement of Railway Ballast. PhD Thesis. University of Nottingham.

Lim and McDowell (2005). Discrete element modelling of railway ballast. Granular Matter, 7(1),19-29.

Lu, M. and McDowell, G.R. (2008). "Discrete element modelling of railway ballast under triaxial conditions." Geomechanics and Geoengineering: An International Journal, 3(4), pp: 257--270.

McDowell, G. R., Harireche, O., Konietzky, H., Brown, S. F., & Thom, N. H. (2006). Discrete element modelling of geogrid-reinforced aggregates. Proceedings of the Institution of Civil Engineers-Geotechnical Engineering, 159(1), 35-48.

Ngo, N. T., 2012, Performance of geogrids stabilized fouled ballast in rail tracks. PhD Thesis, University of Wollongong.

Ngo, N. T., Indraratna, B., & Rujikiatkamjorn, C. (2014). DEM simulation of the behaviour of geogrid stabilised ballast fouled with coal. Computers and Geotechnics, 55, 224-231.

Ngo, N.T., Indraratna, B. and Rujikiatkamjorn, C. (2016). Modelling geogrid-reinforced railway ballast using the discrete element method. Transportation Geotechnics, 8(2016), pp: 86-102.

Ngo, N.T., Indraratna, B. and Rujikiatkamjorn, C. (2017a). A study of the geogrid–subballast interface via experimental evaluation and discrete element modelling. Granular Matter, 19(3), pp: 54-70.

Ngo, N.T., Indraratna, B. and Rujikiatkamjorn, C. (2017b). Simulation ballasted track behavior: Numerical treatment and field application. International Journal of Geomechanics, 17(6), 04016130.

Palmeria, E. M., & Milligan, G. W. E. (1989). Scale and other factors affecting the results of pull-out tests of grids buried in sand. Geotechnique, 39(3), 511-542.

Radjai, F., Wolf, D. E., Jean, M., & Moreau, J. J. (1998). Bimodal character of stress transmission in granular packings. Physical review letters, 80(1), 61.

Raymond, G., & Ismail, I. (2003). The effect of geogrid reinforcement on unbound aggregates. Geotextiles and Geomembranes, 21(6), 355-380.

Rujikiatkamjorn, C., Ngo, N.T., Indraratna, B., Vinod, J. and Coop, M. (2013). Simulation of fresh and fouled ballast behavior using discrete element method. Proceedings of the International Conference on Ground Improvement and Ground Control, (pp. 1585-1592). pp: Singapore: Research Publishing.

Selig, E.T. and Waters, J.M. (1994). Track geotechnology and substructure management, Thomas Telford, London.

Sufian, A., Russell, & Whittle, A. J. (2017). Anisotropy of contact networks in granular media and its influence on mobilised internal friction. Géotechnique, 1-14.

Teixeira, S. H., Bueno, B. S., & Zornberg, J. G. (2007). Pullout resistance of individual longitudinal and transverse geogrid ribs. Journal of geotechnical and geoenvironmental engineering, 133(1), 37-50.

Thornton, C. Antony, J. (1998). Quasi-static deformation of particulate media. Phil. Trans. R. Soc. London A: Math., Phys. Engng Sci. 356, 1747, 2763–2782.

Tutumluer, E., Huang, H. Bian, (2012). Geogrid-aggregate interlock mechanism investigated through aggregate imaging-based discrete element modeling approach. International Journal of Geomechanics, 12(4), 391-398.

Kwon, J. and Penman, J. (2009). The use of biaxial geogrids for enhancing the performance of sub-ballast and ballast layers-previous experience and research. Bearing Capacity of Road, Railways and Airfields Taylor & Francis Group, London.